J Mater Sci: Mater Med (2009) 20:2139–2144
DOI 10.1007/s10856-009-3770-9

Bioglass®-based scaffolds with carbon nanotube coating for bone tissue engineering

Decheng Meng · John Ioannou · Aldo R. Boccaccini

Received: 13 April 2009 / Accepted: 27 April 2009 / Published online: 13 May 2009
© Springer Science+Business Media, LLC 2009

Abstract Highly porous 45S5 Bioglass®-based foam scaffolds were coated with multi-walled carbon nanotubes (CNT) by electrophoretic deposition (EPD) technique. By placing the scaffolds in between the two electrodes of the EPD cell, a CNT coating of up to 1 μm thickness was achieved on the surface throughout the whole three dimensional (3D) matrix. A 0.5 wt% CNT aqueous suspension was used and EPD was carried out at 2.8 V for 10 mins. The compression strength of this CNT/Bioglass® composite was measured to be 0.70 MPa. Moreover the increased electrical conductivity of the composite with CNT coating was confirmed. The scaffolds have the potential for applications in bone tissue engineering due to the high bioactivity, nano-roughness in 3D and electrical conductivity provided by the addition of CNT.

1 Introduction

Bone tissue engineering is a field that involves the principles of biology and engineering to develop viable substitutes that restore and maintain the function of human bone tissues [1]. It requires a porous three-dimensional (3D) matrix (or scaffold) made with biodegradable materials and designed such that it can mimic the bone extracellular matrix (ECM). The goal is for the cells to attach to the scaffold, multiply, differentiate and organize themselves into healthy bone as the scaffold degrades. Bioglass® is one of the most well known and widely used bioactive inorganic materials for bone tissue engineering [2, 3]. The basic constituents of this bioactive glass are SiO_2, Na_2O, CaO, and P_2O_5 [4]. It is highly surface reactive and can rapidly produce a hydroxycarbonated apatite layer that can bond to biological tissue when in contact with relevant biological fluids.

Carbon nanotubes (CNT) are highly ordered nanomaterials that are attracting much attention for a wide range of technology applications [5]. Numerous materials have been combined with carbon nanotubes, including polymers [6], metals [7] and ceramics [8] to form advanced composite materials with enhanced functional and mechanical properties. The properties of these materials have enabled CNT to be applied in many different fields, e.g. biomedical sensors [9], storage of gas [10], electrodes of supercapacitors [11] and field emissions devices [12], besides recent developments on the use of CNT in the biomedical field, which have addressed the biocompatibility between cells and CNT for tissue engineering [13, 14].

Electrophoretic deposition (EPD) has been shown to be one of the most effective methods to manipulate CNT and to produce ordered macroscopic CNT assemblies [15]. In this technique, charged particles suspended in a liquid medium migrate under the influence of an electric field (electrophoresis) and are deposited onto an electrode [16].

As reviewed elsewhere [17], EPD is a promising technique for nanomaterial processing, because it involves simple equipment, low fabrication costs, short formation time and few substrates' shape restrictions. EPD is very useful to produce coatings and films of homogeneous microstructure and controlled thickness on a wide variety of substrates of different shape and dimensions [17].

Among the first researchers to develop EPD of CNT, Du et al. [18] demonstrated the deposition of CNT on metallic substrates by EPD using ethanol/acetone as

D. Meng · J. Ioannou · A. R. Boccaccini (✉)
Department of Materials, Imperial College London,
Prince Consort Road, London SW7 2AZ, UK
e-mail: a.boccaccini@imperial.ac.uk

solvents. An extensive review describing the different solvent systems and EPD parameters used for deposition of ordered arrays of CNTs has been published elsewhere [15]. Most previous work, however, has focused on CNT deposition on planar substrates. It has been previously reported [19] that EPD can also be applied to produce uniform CNT coatings on the surfaces of 3D highly porous bioactive glass scaffolds without impairing the scaffold bioactivity. It was observed that the presence of CNT can induce the ordered formation of a nanostructured CNT/HA composite layer when the substrates are immersed in simulated body fluid [19].

However a comprehensive characterisation of novel CNT coated Bioglass® scaffolds has not been carried out as yet. The addition of CNT to a bioactive tissue engineering scaffold represents the opportunity to develop 'smart' scaffolds, which will exhibit an electrically conductive nanostructured fibrous surface layer and improved mechanical properties by EPD [20, 21].

In this work, we investigate the CNT coating on porous Bioglass®-based scaffolds using a novel CNT suspension system and, for the first time, we characterise the compressive strength of the coated scaffolds, showing also the evidence of electrical conductivity of the composite, aiming at improving cell–cell interaction during cell attachment and proliferation.

2 Experiments

45S5 Bioglass® powder (particle size $\leq$10 μm) was kindly supplied by Dr. I. Thompson (Kings College London, UK). A commercial CNT suspension, AquaCyl™ (AQ0101), was purchased from Nanocyl (Belgium), and it was used as received. The zeta-potential of Bioglass® particles in aqueous suspension was measured using an Agilent 7020 ZetaProbe (Foster City, USA). The zeta-potential of the CNT suspension was measured using a ZetaPALS zeta Potential Analyzer (Brookhaven, Inst. Corp, Holtsville, USA). Different concentrations of the CNT suspension were diluted with distilled water. Both the foam-replication method used for scaffold fabrication and the simulated body fluid (SBF) immersion method to investigate bioactivity were described previously [22]. Briefly, a slurry was prepared adding 40 wt% Bioglass® particles and 6 wt% polyvinyl acetate in water. To fabricate the scaffolds, a polyurethane (PU) foam (45 ppi, pores per inch, Recticel, Corby, UK) was immersed and squeezed in the slurry, which consequently infiltrates the foam structure and glass particles adhere to the surfaces of the polymer foam. Extra slurry was squeezed out vigorously by hand after the foam had been taken out of the slurry to give a reasonably homogeneous coating (assessed by visual inspection). After drying the coated PU foam at 60°C for 12 h, it was sintered at 1100°C for 2 h [22] to produce a partially crystallized Bioglass®-based scaffold.

Figure 1 shows a SEM image of a typical Bioglass® derived scaffold used in this research. The CNT coating on scaffolds was achieved using EPD. A scaffold was hanged using a copper wire between the two electrodes in the EPD cell. The electrodes were made of stainless steel 316L foil with dimension of $20 \times 10 \times 0.02$ mm^3. The separation distance between electrodes was 20 mm. The electrodes were connected to a DC power supply and a constant voltage was applied when the scaffold and electrodes were lowered into the CNT suspension. After certain time period, the scaffold and electrodes were withdrawn from the CNT suspension slowly in order to avoid the influence of the drag force between the suspension and the deposited wet CNT coating, which could lead to disruption of the coating. Finally, the scaffold was left to dry at room temperature in air.

The scaffold samples were characterised by SEM (JEOL 5610LV) and X-ray diffraction (XRD), (Phillips PW 1700 Series automated powder diffractometer). XRD was carried out using Cu Kα radiation of 40 kV and 40 mA, in the 2θ range 5–80°, step size of 0.04° and counting time of 2 s.

The compressive strength of composite scaffolds was tested by using a Zwick/Roell Z010 universal testing machine. All scaffolds were carefully shaped into prismatic specimens of dimensions $5 \times 5 \times 10$ mm^3, and then coated with CNT using EPD. The load was applied on the 5×5 mm^2 face. The cross-head speed was 0.5 mm/min. The load was applied until the compressive strain reached the value of 70%. Teflon® film of 0.05 mm in thickness was used to cover the bottom and top loading platens of the testing machine to prevent the sample from misalignment.

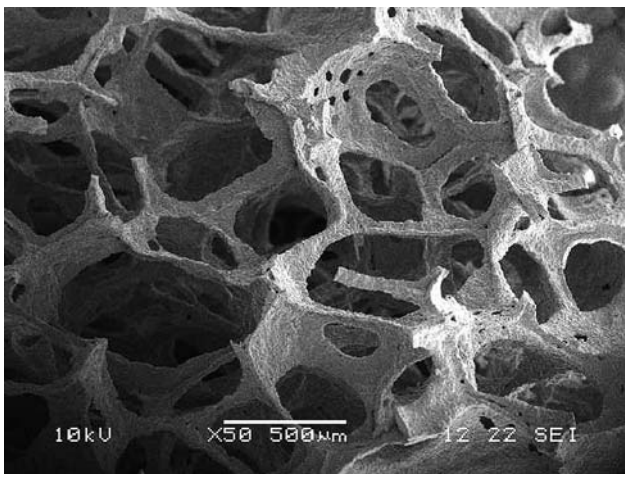

Fig. 1 SEM micrograph showing the 3D microstructure of the highly porous glass–ceramic scaffold developed from Bioglass® powder by the foam replica technique

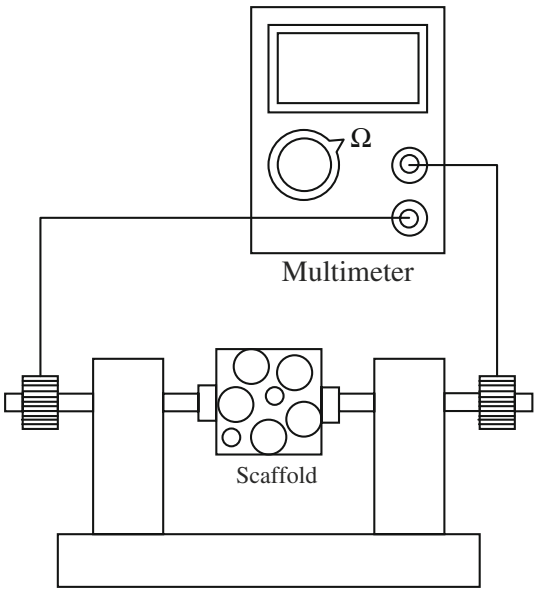

Fig. 2 Schematic diagram showing the device to measure the electrical resistance of CNT-coated scaffolds

The electrical resistance of CNT-coated scaffolds was measured using a FLUKE 77 Series II Multimeter. The scaffold was connected to the multimeter by a spring loaded device; a schematic diagram of the experimental set up used for these measurements is shown in Fig. 2.

3 Results and discussion

In order to determine whether or not the CNT would deposit onto the 3D Bioglass® scaffold, the surface charges of both materials (CNT and Bioglass® particles) in aqueous suspension were analysed. The pH dependent zeta-potential curves of the two materials are shown in Fig. 3. The

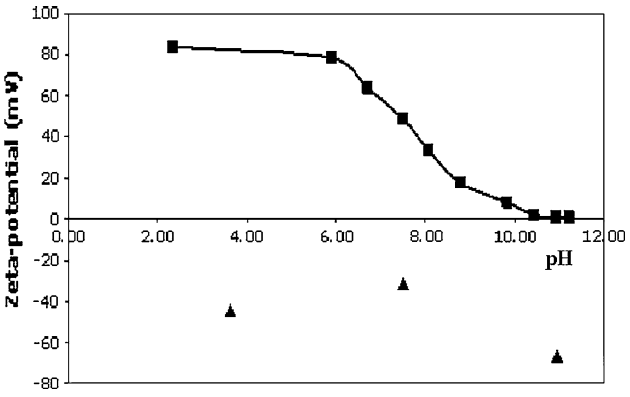

Fig. 3 Zeta-potential versus pH relationship for Bioglass® particles and CNT in aqueous suspensions (*filled square*, Bioglass®; *filled triangle*, CNT)

initial pH of the CNT suspension is 11, and the zeta-potential of CNT was determined to be −66.97 mV at that point, while Bioglass® particles were seen to be slightly positively charged, although close to the isoelectric point. Hence, in principle, if a 45S5 Bioglass® scaffold is suspended in-between the two electrodes in the EPD cell, as done in the present EPD experiments, the negatively charged CNT will migrate to the anode and pass through the porous structure of the scaffold, thus a significant amount of these migrating CNTs will deposit both onto the external and internal surfaces of the scaffold; creating a fairly homogeneous CNT coating throughout the 3D porous matrix (shown in Fig. 1).

Three concentrations of CNT aqueous suspensions were investigated. These were 1.0 (initial concentration), 0.5, and 0.25 wt%. EPD was carried out for 5 min, 10, 15, and 20 min. All EPD experiments were performed at 2.8 V in order to minimise bubble formation due to the electrolysis of water.

It was found that the 1 wt% CNT suspension was too viscous and it blocked the pores of the scaffold once the composite was dried. This effect is undesirable since the scaffold porosity must be kept at a high level (see Fig. 1) for cellular nutrients transfer and vascularisation requirements in in vivo conditions [23]. Homogeneous coatings could not be achieved using the 0.25 wt% CNT suspension due to the low CNT concentration as determined by SEM. On the other hand, the 0.5 wt% CNT suspension was found to provide qualitatively the best result, as a fairly even CNT coating of around 1 μm thickness (determined by SEM) was obtained by a 10 min EPD process, as shown in Fig. 4.

The mechanical behaviour of the CNT coated scaffolds was investigated by testing their compressive strength. Five samples from each EPD condition, using 0.5 and 0.25 wt% CNT suspensions, were tested and the average values were taken. For the 0.5 wt% CNT suspension, the average compression strength was 0.70 ± 0.03 MPa, and for the 0.25 wt% CNT suspension, it was 0.50 ± 0.05 MPa. Non-coated samples exhibited a compressive strength of 0.65 ± 0.04 MPa, indicating that the CNT coating did not improve the scaffold compressive strength. This is because the CNT are only deposited on the surface of the scaffold forming a superficial layer; hence they cannot act as reinforcement of the brittle foam struts. The possibility of fabricating scaffolds with CNT embedded in the glass–ceramic matrix is being investigated.

The formation of hydroxyapatite (HA) on the surface of 45S5 Bioglass® scaffolds after immersion in SBF is commonly used as the marker for the scaffold bioactivity [4, 22]. After immersing different scaffolds in SBF for 1 week (including non-coated scaffolds, 1 wt% CNT suspension coated scaffolds and 0.5 wt% CNT suspension

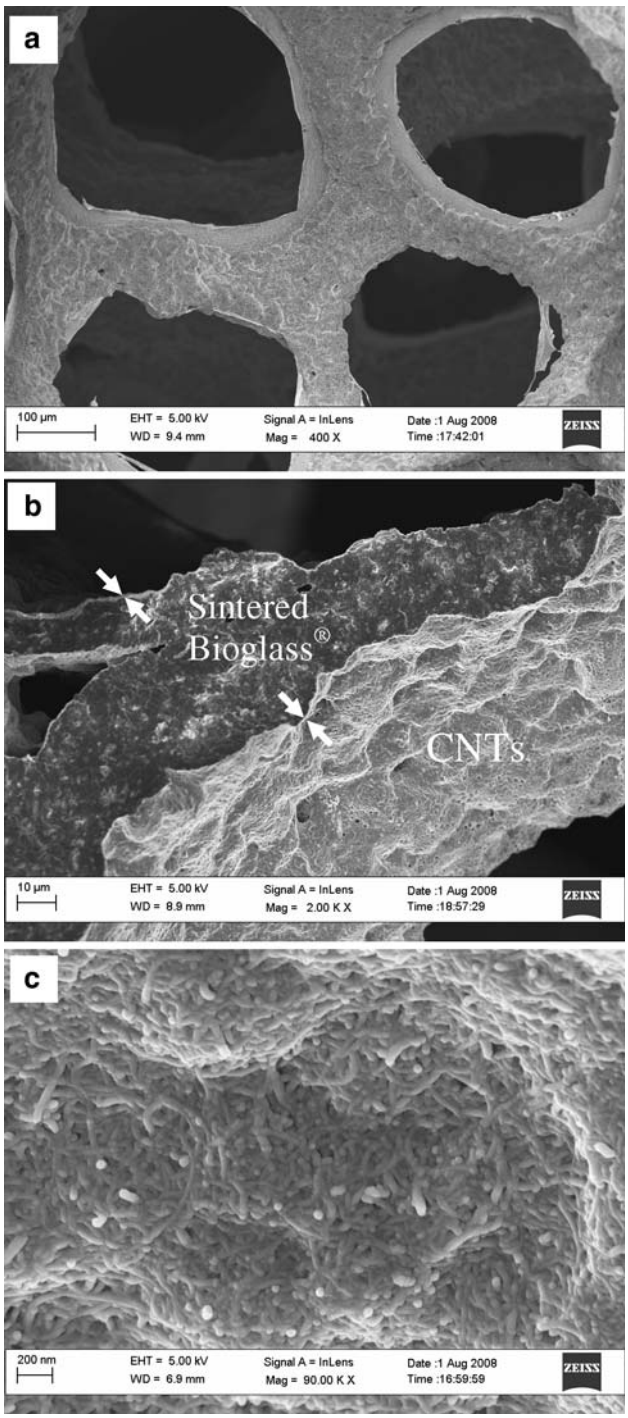

Fig. 4 SEM images showing the typical microstructure of a CNT coated scaffold, obtained by EPD (2.8 V, 10 min) at **a** low, **b** medium and **c** high magnifications. The CNT coating is indicated by the arrows in (**b**)

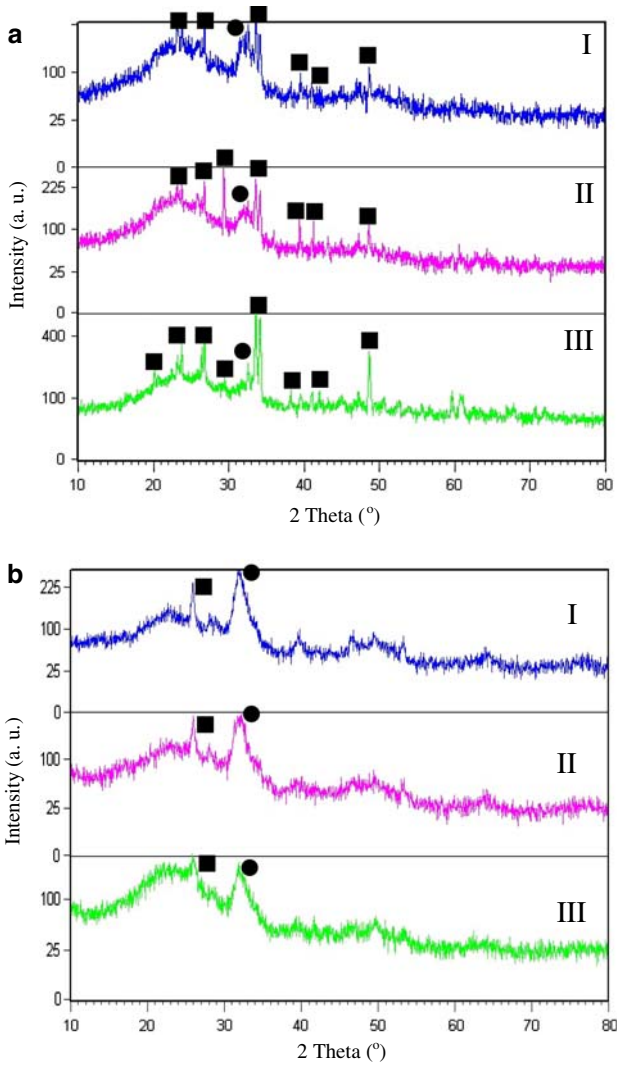

Fig. 5 Comparison of XRD results on CNT-coated and uncoated Bioglass®-based scaffold samples that have been immersed in SBF for **a** 1 week and **b** 4 weeks at 37°C. (I) Uncoated scaffold; (II) 0.5 wt% CNT suspension coated scaffold, (III) 1.0 wt% CNT suspension coated scaffold (*filled square*, $Na_2Ca_2Si_3O_9$, crystalline phase developed in the sintered Bioglass® struts; *filled circle*, HA)

coated scaffolds), the influence of the presence of CNT on HA formation was monitored using SEM and XRD analyses. It was observed that HA peaks appear in the XRD spectra of scaffolds after 1 week immersion in SBF, they are marked as dots in Fig. 5a. One can observe that the intensity of the HA peaks is strongest for the non-coated sample (Fig. 5aI), while the spectrum of the 1 wt% CNT suspension coated sample (Fig. 5aIII) is mainly dominated by the sodium calcium silicate phase, $Na_2Ca_2Si_3O_9$ (the crystalline phase present in the glass–ceramic scaffold after sintering [22]), which means that the bioactivity of the scaffold was slowed down at the early stages of immersion in SBF by the presence of the CNT coating. However, after 4 weeks in SBF, all samples showed very similar intensity of the HA peaks in their XRD spectra, and $Na_2Ca_2Si_3O_9$ peaks almost completely disappeared (Fig. 5b). SEM images (Fig. 6) of a CNT coated scaffold (using the 0.5 wt% CNT suspension) show that after 4 weeks of immersion in SBF, homogenously formed HA crystals

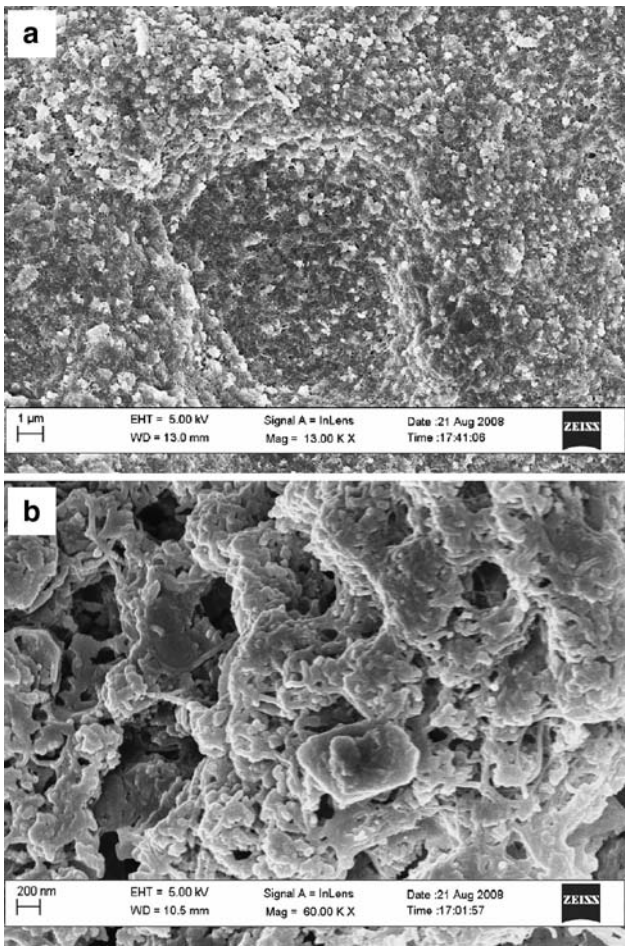

Fig. 6 **a** SEM image of a 0.5%wt CNT suspension coated Bioglass®-based scaffold after 4 weeks of immersion in SBF, showing uniform development of submicrometric HA crystals, which are shown in detail in the higher magnification image (**b**)

have developed in contact with the CNT coating. Therefore, bioactivity, i.e. confirmed by the formation of HA, was promisingly observed on the 0.5 wt% CNT suspension coated Bioglass® scaffolds. More encouraging, no large agglomerates of needle-like HA crystallites were observed on the surface of the CNT coated scaffolds (which are commonly seen on uncoated scaffolds, e.g. see ref. [22]). Thus, one can conclude that the addition of a CNT coating has contributed to create a homogenous nanoscale HA layer by acting as a separating surface-mesh or template, thus preventing HA crystallites from uncontrolled agglomeration. The formation of a nanoscale HA/CNT surface structure should be beneficial for cell attachment on these scaffolds [13, 14, 24].

The electrical conductivity of the scaffold was determined by using a multimeter. Only the 0.5 wt% CNT suspension coated scaffold was measured since this scaffold type exhibited the optimised CNT structure, as discussed above. The average of 20 readings (measured on different locations of the outer walls of the scaffold) was 10,375 Ω, which is notably lower than the value of the uncoated scaffold, which could not be measured due to its extremely high value (Bioglass® being an insulator) exceeding the range of measurement of the instrument used.

The incorporation of CNT to develop conductive scaffolds may aid in directing cell growth [25–27]. For instance, in the case of bone regeneration and fracture healing the use of an electric field is based on the observation that, when bone is subjected to mechanical stresses, deformation of bone is normally accompanied by an electrical signal bearing the strain characteristics [26]. Therefore, an electrically conductive scaffold, e.g. incorporating carbon nanotubes, can potentially be used for stimulating cell growth and bone tissue regeneration by facilitating the physioelectrical signal transfer [27].

4 Conclusions

A uniform, multi-walled CNT coating was achieved throughout 3D 45S5 Bioglass®-based glass–ceramic scaffolds by electrophoretic deposition. A thickness of up to 1 µm of the CNT coating was obtained, using a commercially available CNT suspension at 2.8 V for 10 mins. The scaffold mechanical strength and bioactivity were not impaired by the presence of CNT. The addition of CNT imparted electrical conductivity to the otherwise insulating 3D scaffolds. CNT-coated scaffolds are promising model systems to test the interaction of cells with nanofibrous 3D bioactive substrates and to investigate for the first time the effect of electrical conduction in 3D matrices on cellular behaviour.

Acknowledgment The authors thank Dr. Sasa Novak, Ms. Katja Koenig and Ms. Katja Rade (Jozef Stefan Institute, Slovenia) for experimental support during zeta potential measurements and the British Council for partial financial support.

References

1. Chaikof EL, Matthew H, Kohn J, Mikos AG, Prestwich GD, Yip CM. Biomaterials and scaffolds in reparative medicine. Ann N Y Acad Sci. 2002;961:96–105.
2. Xynos ID, Edgar AJ, Buttery LDK, Hench LL, Polak M. Gene-expression profiling of human osteoblasts following treatment with the ionic products of Bioglass 45S5 dissolution. J Biomed Mater Res. 2001;55:151–7. doi:10.1002/1097-4636(200105)55:2<151::AID-JBM1001>3.0.CO;2-D.
3. Rezwan K, Chen QZ, Blaker JJ, Boccaccini AR. Biodegradable and bioactive porous polymer/inorganic composite scaffolds for bone tissue engineering. Biomaterials. 2006;27(18):3413–31. doi:10.1016/j.biomaterials.2006.01.039.
4. Hench LL. Bioceramics. J Am Ceram Soc. 1998;81(7):1705–28.
5. Meyyappan M. Carbon nanotubes: science and applications. London, UK: CRC Press; 2004.

6. Jin L, Bower C, Zhou O. Alignment of carbon nanotubes in a polymer matrix by mechanical stretching. Appl Phys Lett. 1998;73(9):1197–9. doi:10.1063/1.122125.
7. Gao CL. Ordered arrays of magnetic metal nanotubes and nanowires encapsulated with carbon tubes. J Nanosci Nanotechnol. 2008;8(9):4494–9. doi:10.1166/jnn.2008.307.
8. Hwang GL, Hwang KC. Carbon nanotube reinforced ceramics. J Mater Chem. 2001;11(6):1722–5. doi:10.1039/b101294k.
9. Lin Y. Advances toward bioapplications of carbon nanotubes. J Mater Chem. 2004;14(4):527–41. doi:10.1039/b314481j.
10. Guay P, Stansfield BL, Rochefort A. On the control of carbon nanostructures for hydrogen storage applications. Carbon. 2004;42(11):2187–93. doi:10.1016/j.carbon.2004.04.027.
11. Frackowiak E. Supercapacitors based on conducting polymers/nanotubes composites. J Power Sources. 2006;153(2):413–8. doi:10.1016/j.jpowsour.2005.05.030.
12. Bae JC. Field emission properties of carbon nanotubes deposited by electrophoresis. Physica B. 2002;323(1–4):168–70. doi:10.1016/S0921-4526(02)00890-6.
13. Mwenifumbo S, Shaffer MS, Stevens MM. Exploring cellular behaviour with multi-walled carbon nanotube constructs. J Mater Chem. 2007;17(19):1894–902. doi:10.1039/b617708e.
14. Zanello LP. Bone cell proliferation on carbon nanotubes. Nano Lett. 2006;6(3):562–7. doi:10.1021/nl051861e.
15. Boccaccini AR, Cho J, Roether JA, Thomas BJC, Minay EJ, Shaffer MSP. Electrophoretic deposition of carbon nanotubes—a review. Carbon. 2006;44:3149–60. doi:10.1016/j.carbon.2006.06.021.
16. Sarkar P, Nicholson PS. Electrophoretic deposition (EPD): mechanisms, kinetics, and application to ceramics. J Am Ceram Soc. 1996;79(8):1987–2002. doi:10.1111/j.1151-2916.1996.tb08929.x.
17. Boccaccini AR, Zhitomirsky I. Application of electrophoretic and electrolytic deposition techniques in ceramics processing. Curr Opin Solid State Mater Sci. 2002;6(3):251–60. doi:10.1016/S1359-0286(02)00080-3.
18. Du CS, Heldbrant D, Pan N. Preparation and preliminary property study of carbon nanotubes films by electrophoretic deposition. Mater Lett. 2002;57(2):434–8. doi:10.1016/S0167-577X(02)00806-6.
19. Boccaccini AR, Chicatun F, Cho J, Bretcanu O, Roether JA, Novak S, et al. Carbon nanotube coatings on bioglass-based tissue engineering scaffolds. Adv Funct Mater. 2007;17(15):2815–22. doi:10.1002/adfm.200600887.
20. White AA, Best SM, Kinloch IA. Hydroxyapatite–carbon nanotube composites for biomedical applications: a review. Int J Appl Ceram Technol. 2007;4:1–13. doi:10.1111/j.1744-7402.2007.02113.x.
21. MacDonald RA, Laurenzi BF, Viswanathan G, Ajayan PM, Stegemann JP. Collagen-carbon nanotube composite materials as scaffolds in tissue engineering. J Biomed Mater Res A. 2005;74:489–95.
22. Chen QZ, Thompson ID, Boccaccini AR. 45S5 Bioglass-derived glass-ceramic scaffolds for bone tissue engineering. Biomaterials. 2006;27(11):2414–25. doi:10.1016/j.biomaterials.2005.11.025.
23. Karageorgiou V, Kaplan D. Porosity of 3D biomaterial scaffolds and osteogenesis. Biomaterials. 2005;26(27):5474–91. doi:10.1016/j.biomaterials.2005.02.002.
24. Webster TJ, Ahn ES. Nanostructured biomaterials for tissue engineering bone. Adv Biochem Eng Biotechnol. 2007;103:275–308. doi:10.1007/10_021.
25. Zhang D, Kandadai MA, Cech J, Roth S, Curran SA. Poly(L-lactide) (PLLA)/multiwalled carbon nanotube (MWCNT) composite: characterization and biocompatibility evaluation. J Phys Chem B. 2006;110:12910–5. doi:10.1021/jp061628k.
26. Aaron RK, Boyan BD, Ciombor DM, Schwartz Z, Simon BJ. Treatment of nonunions with electric and electromagnetic fields. Clin Orthop Relat Res. 2004;419:21–9. doi:10.1097/00003086-200402000-00005.
27. Supronowicz PR, Ajayan PM, Ullmann KR, Arulanandam BP, Metzger DW, Bizios R. Novel current-conducting composite substrates for exposing osteoblasts to alternating current stimulation. J Biomed Mater Res. 2002;59:499–506. doi:10.1002/jbm.10015.